ALTIGLACIO - Marché sous accord-cadre n°180579

Lot 1-task 1.1: mono-mission sea level in the Arctic Ocean

Reference:	CLS-ENV-NT-19-0341
Nomenclature:	-
Issue:	1. 2
Date:	2019,Aug.26

CLS headquarters
11 rue Hermès
Parc technologique du Canal
31520 Ramonville Saint-Agne
FRANCE

Tel. +33 (0)5 61 39 47 00
Fax +33 (0)5 61 75 10 14
Mail: info@cls.fr
www.cls.fr

CLS Brest Le Ponant
Zone du technopôle de Brest Iroise
Avenue La Pérouse
29280 Plouzané
FRANCE

Tel. 33 (0)2.98.05.76.80
Fax 33 (0)2.98.05.76.90

Chronology Issues:

Issue:	Date:	Reason for change:	Author
1.0	26/08/19	Creation	P. Prandi
1.1	3/10/19	Response to reviews	P. Prandi
1.2	17/11/19	Add reference to Poisson et al. paper	P. Prandi

People involved in this issue:

Written by (*):	P. Prandi	Date + Initials:(visa or ref)
Checked by (*):	NA	Date + Initial:(visa ou ref) [Checker]
Approved by (*):	NA	Date + Initial:(visa ou ref) [Approver]
Application authorized by (*):	NA	Date + Initial:(visa ou ref)

In the opposite box: Last and First name of the person + company if different from CLS

Index Sheet:

Context:	
Keywords:	[Mots clés]
Hyperlink:	

Distribution:

Company	Means of distribution	Names
CLS	Notification	P. Prandi, P. Thibaut, Y. Faugère, J-C. Poisson
CNES	Notification	A. Guillot.

FORM-NT-GB-10-1

List of tables and figures

List of tables:

List of figures:

List of items to be confirmed or to be defined

Lists of TBC:

Aucune entrée de table des matières n'a été trouvée.

Lists of TBD:

Aucune entrée de table des matières n'a été trouvée.

Applicable documents

AD 1 Plan d'assurance produit de CLS
CLS-ED-NT-03-394

Reference documents

RD 1 Manuel du processus Documentation
CLS-DOC

RD 2 Armitage, T. W. K., Bacon, S., Ridout, A. L., Thomas, S. F., Aksenov, Y., and Wingham, D. J. (2016), Arctic sea surface height variability and change from satellite radar altimetry and GRACE, 2003–2014, J. Geophys. Res. Oceans, 121, 4303– 4322, doi:10.1002/2015JC011579

RD 3 Proshutinsky, A. Y., and Johnson, M. A. (1997), Two circulation regimes of the wind-driven Arctic Ocean, J. Geophys. Res., 102(C6), 12493– 12514, doi:10.1029/97JC00738.

RD 4 Stine Kildegaard Rose, Ole Baltazar Andersen, Marcello Passaro, Carsten Ankjær Ludwigsen andChristian Schwatke, Arctic Ocean Sea Level Record from the Complete Radar Altimetry Era: 1991–2018, Remote Sens. 2019, 11(14), 1672; https://doi.org/10.3390/rs11141672

RD 5 Peacock, N. R. and Laxon, S., Sea surface height determination in the Arctic Ocean from ERS altimetry, JGR-Oceans, 2004, 109

RD 6 Poisson, J.C.; Quartly, G.D.; Kurekin, A.A.; Thibaut, P.; Hoang, D.; Nencioli, F. Development of an ENVISAT altimetry processor providing sea level continuity between open ocean and Arctic leads. IEEE Trans. Geosci. Remote Sens. 2018, 56, 5299–5319.

List of Contents

1. Introduction

The present document summarizes the studies performed in the frame of the CNES AltiDoppler glaciologie 2018 contract (n°180579), lot 1, task 1.1 to estimate sea surface height from radar altimeter measurements in the Arctic Ocean.
Here we address mono-mission analysis only, from SARAL/AltiKa, Sentinel-3A and CryoSat-2 measurements.

The first complete Arctic Ocean dataset can be traced back to Peacock and Laxon, 2004 (RD 5) who used ERS altimetry data and provided the first map of sea level variability of the Arctic Ocean. The launch of CryoSat-2, which observes the polar ocean up to 89.5°N, has increased the polar ocean coverage and lead to the development of new Arctic sea level products. The current reference is the work performed by Armitage *et al.*, 2016 (RD 2), who used CryoSat-2 data to estimate large-scale dynamic ocean topography features at a monthly resolution. Recently, Rose et al. (RD 4) published a new Arctic Ocean dataset which covers the whole satellite radar altimeter period since the launch of ERS-1.

At CLS, previous work lead to the generation of Arctic Ocean sea level datasets based on Envisat and SARAL/AltiKa, as part of the ESA SL-CCI and CNES PEACHI projects respectively.

In this document we describe the data processing scheme used to generate sea level anomaly grids for the Arctic Ocean from along-track radar altimeter measurements. The datasets generated here serve several purposes:

- Expand the time span of previous datasets based on Envisat and SARAL/AltiKa measurements,
- Adapt the LRM processing chain to SAR altimeter data from Sentinel-3A and CryoSat-2,
- Provide sea level data over the same area and period and perform intercomparisons,
- Prepare a multi-mission combination analysis.

2. Data processing overview

The data processing is summarized in the chart below. After echo retracking and classification, we select open ocean and lead echoes only. Applying standard geophysical corrections results in along-track sea level anomaly measurements. An editing is then applied to remove erroneous measurements and data outliers. Valid along-track measurements are then binned to construct the final gridded product.
The different processing steps are detailed in separate sections below and when needed, processing differences between missions are highlighted.

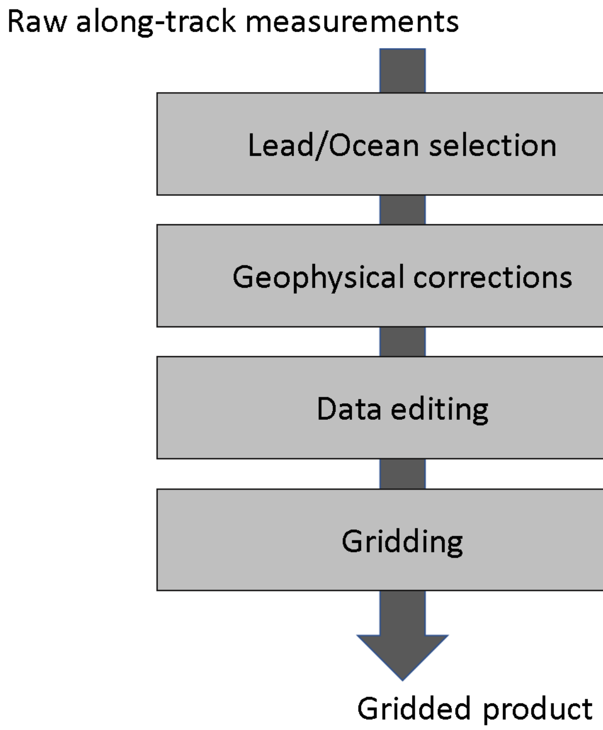

Figure 1, data processing overview

3. Periods

Data availability differs for different missions, and the final products unfortunately do not cover exactly the same time span. Far all three missions, the start and end of the timespan are given in Table 1. This represents three years for SARAL/AltiKa and two years for Sentinel-3A and CryoSat-2. The overlap period where all three missions are available is 1.5 years long.

	Start	End
SARAL/AltiKa	2016/01/01	2018/12/31
Sentinel-3A	2016/06/30	2018/06/19
CryoSat-2	2016/01/01	2018/12/31

Table 1, start and end dates for the three missions considered in this study

4. Data pre-processing

For SARAL/AltiKa and Sentinel-3A data, we rely on L2E-HR databases to perform this work. In this case, the only preprocessing step required is to perform a copy from L2E-HR global databases to extract the region of interest.
For CryoSat-2, there is no PDGS Ice based L2E-HR database that covers the region of interest over the full period, therefore a regional Arctic database is created from Ice SAR L1b products distributed by ESA. These include 0-padding/Hamming windowing of the waveforms.

Several acquisition and update steps are required before the application of the SLA retrieval processing chain, these include:
- Acquisition,
- Update of attitude parameters,
- Update of the relative tracker,
- Classification,
- Retracking.

4.1. Retracking

In this study, we deal with different altimeter modes (LRM and SAR) and different processings. For SARAL/AltiKa and Sentinel-3A data, we rely on L2E-HR databases to build regional “L2P-HR” databases. Details of the instrument retracking are listed below for the three missions considered.

4.1.1. SARAL/AltiKa

We rely on the latest version of the Adaptive retracking algorithm [RD 6]. All echoes (ocean and leads) are processed with the same algorithm at L2E-HR level.

4.1.2. Sentinel-3A

Again, we rely on L2E-HR data coming from the CNES S3PP processor in its 0-pad + Hamming version. For leads we use the TFMRA retracker outputs and a standard MLE retracker for Brownian echoes. Both are available in L2E-HR databases. The retracking threshold for the TFMRA retracker is set to 80%.

4.1.3. CryoSat-2

No L2E-HR database was available for CryoSat-2 based on PDGS SAR ICE products. The regional CryoSat-2 database was recreated for this study from level 1b products. We run the TFMRA retracking on all echoes and perform the classification. As a result, the area observed by CryoSat-2 is limited by the mode mask, which roughly follows the ice extent. The retracking threshold for the TFMRA retracker is set to 50%.

5. Lead/Ocean selection

Over the Arctic Ocean echoes acquired by altimeters show a wide variety of shapes, with large deviations from the classical Brownian echo shape. The variety reflects the variety of surface roughness: open ocean, fast ice, ridged ice, different snow types, and leads that act as bright targets.
For the retrieval of sea level anomaly, we need to select only returns coming from the open ocean and from leads, where we assume that the ocean underneath the ice appears.
The standard practice in the literature is to select lead echoes based on pulse peakiness: a high pulse peakiness is associated with a low roughness surface which

is assumed to be a lead. Here we take advantage of previous work on echo classification to perform this selection. Fortunately, a classification algorithm is available for all missions considered in this study [RD 6].
The decision tree to discriminate between ocean and leads echoes is summarized in the chart below.
Sea ice concentration from OSI-SAF is used first. In areas where SIC lower than 30%, all Brownian (corresponding to class 1) echoes are assigned to open ocean, while all other measurements are discarded from further analysis. In areas where the ice concentration is greater than 30%, peaky echoes (corresponding to class 2) with a backscatter coefficient greater than a given threshold are assigned to leads, all other echoes are rejected.
The backscattering threshold is mission dependent and the thresholds used are summarized in Table 2.

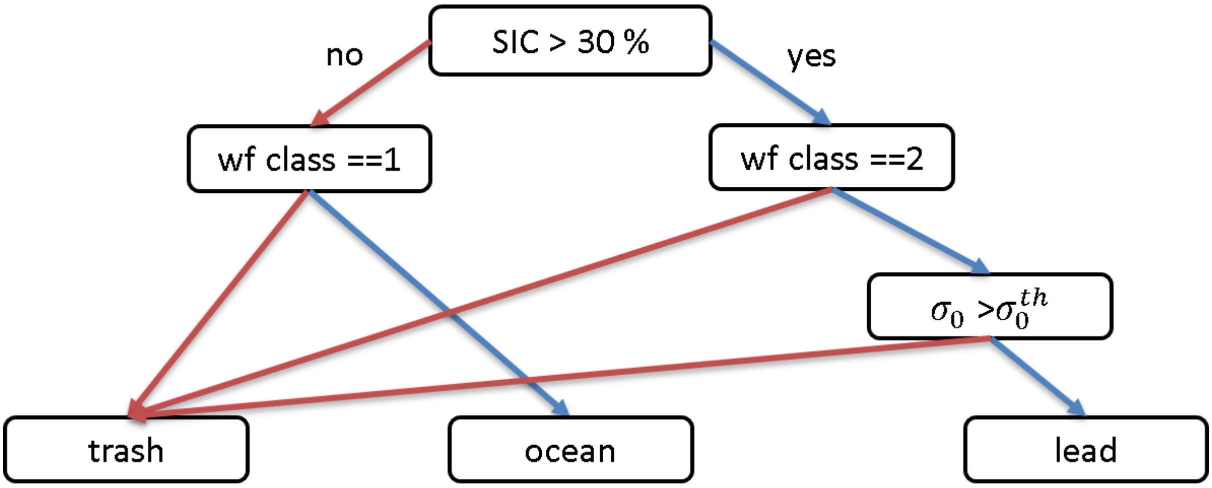

Figure 2, lead and open ocean echoes selection chart

	SARAL/AltiKa	Sentinel-3A	CryoSat-2
Backscatter threshold	20	13	23

Table 2, backscattering thresholds used for the selection of lead echoes

An exemple of the geographical distribution of leads is given on Figure 3 for SARAL/AltiKa, Sentinel-3A and CryoSat-2. This metric is reliable for SARAL and Sentinel-3A only. For CryoSat-2, we discard waveforms with classes different from 1 (ocean) and 2 (peaky) in order to reduce computing time and storage space and ratios are therefore biased, yet this provide a qualitative validation of the selection algorithm.

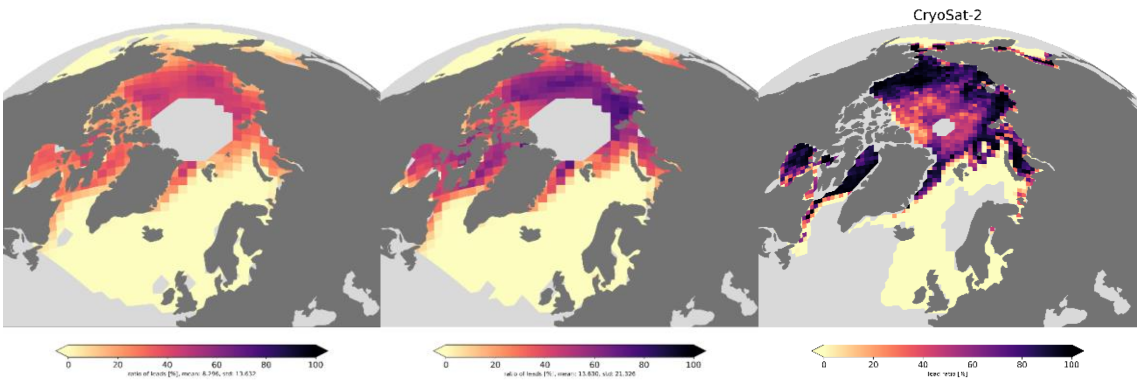

Figure 3, Ratio of measurements considered as leads for SARAL, Sentinel-3A and CryoSat-2

6. Geophysical corrections

Geophysical corrections are mandatory to convert orbit minus range values to sea surface heights and sea level anomaly. The corrections used in this study are listed in the table below.

	SARAL/AltiKa	Sentinel-3A	CryoSat-2
Ocean tide	FES14		
Load tide	FES14		
Pole tide	Desai, 2015		
Solid earth tide	Cartwright and Tayler		
Wet tropo	ECMWF model		
Dry tropo	ECMWF model		
DAC	MOG2D		
Sea state bias	L2E-HR		None
Ionosphere	GIM model		
Mean sea surface	DTU 15		

Please note that the sea state bias is applied only on ocean measurements. We consider that leads are smooth surfaces and do not apply any sea state correction on leads measurements.

7. Data editing

The data editing is a key step in the generation of the Arctic SLA dataset. The editing derives from an important knowledge base available at CLS (based on Cal/Val studies mainly), and from many trials and errors. Editing procedures are difficult to design and to validate. They result from a trade-off between data quality and data coverage. Here we clearly stand on the data coverage side: we are willing to accept lower quality data if it provides what looks like consistent information about the large-scale features of the ice-covered Arctic Ocean variability.

For the generation of this mono-mission SLA dataset, the editing consists in three main steps:

- Check that previous data processing did not encounter any problems, and basic outlier detection,
- Apply and iterative editing on open ocean surfaces,
- Perform an outlier detection based on the expected SLA distribution at a given time/space position.

7.1. Hooking flag

With leads acting as bright targets in the altimeter footprint, several consecutive measurements can stay hooked on the same ground point as the altimeter flies above it, resulting in negative SLA biases.
The hooking detection algorithm is based on local along-track backscattering variations: only the measurement with maximum backscatter is selected inside a moving window. In theory the size of the mowing window should be consistent with the altimeter footprint, in practice such a choice results in a very low valid data ratio, and we select much smaller window width.
As shown on Figure 4, applying the hooking algorithm is very severe in terms of edited measurements, with about 70% of measurements which are considered as hooked, and removed from further analysis.
Theoretically this affects LRM measurements, and the hooking detection algorithm is applied on SARAL/AltiKa data only.
On SARAL/AltiKa, following previous PEACHI work, we use a 7 measurements wide moving window.

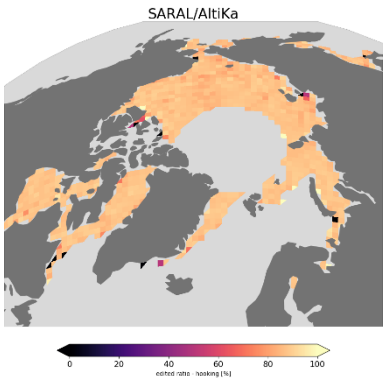

Figure 4, ratio of hooked measurement on SARAL/AltiKa

7.2. Basic thresholding

The first step of the editing procedure is to apply basic checks on several parameters (mission dependent) and a very naïve outlier detection by removing any SLA excursions greater than 2 meters. Figure 2 displays the ratio of edited measurements by this first editing step. Over ice areas, this is already a very strict editing: depending on the mission, 60 to 90% of measurements are edited. This edits almost no measurements over open ocean areas. Note that over sea-ice these numbers include the lead selection process (selection on waveform classification and backscatter).

The editing ratio difference between SARAL/AltiKa and Sentinel-3 is a result of the hooking flag applied on LRM data only.
CryoSat-2 numbers are not directly comparable to the two other missions, as all waveforms that are not classified as 'peaky' (class number 2) or 'brownian' (class number 1) are discarded early in the process to reduce computing time.

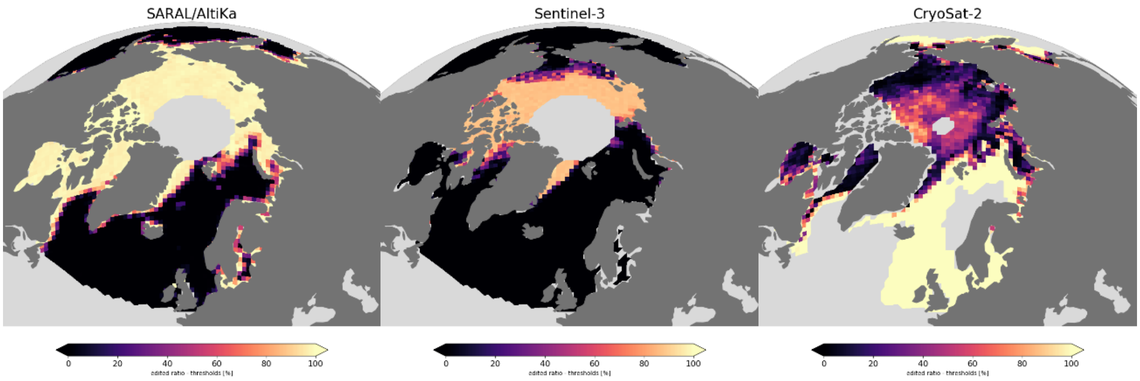

Figure 5, ratio of edited measurements for SARAL/AltiKa, Sentinel-3 and CryoSat-2, expressed in percentage

Details of thresholds applied on different missions are detailed below:

- SARAL/AltiKa
  - valid adaptive retracking
  - no waveform saturation
  - mean quadratic error less than 0.005
  - no hooking
- Sentinel-3A
  - Valid retracking
- CryoSat-2
  - Valid retracking
  - Leads only

For all missions, we also remove any measurements where the SLA is greater than 2 meters.

7.3. Iterative editing

Next we apply an iterative editing procedure which is a standard algorithm to edit high-frequency SLA data. Over a short along-track window, any measurement that departs from the estimated low-frequency SLA is removed from further analysis. While the iterative algorithm is applied on all measurements, its results are considered only on open ocean.
It is worth noting that iterative editing does provide a filtered SLA in addition to the validity flag. This filtered SLA is not used in the SLA analysis.
Over the ice-covered ocean, along-track segments have many gaps which prevent any accurate filtering, as a result the iterative editing applied over sea-ice tends to largely over-edit data (almost all measurements are rejected).

The design and tuning of an editing procedure like the current iterative editing process for leads could provide data quality improvements.

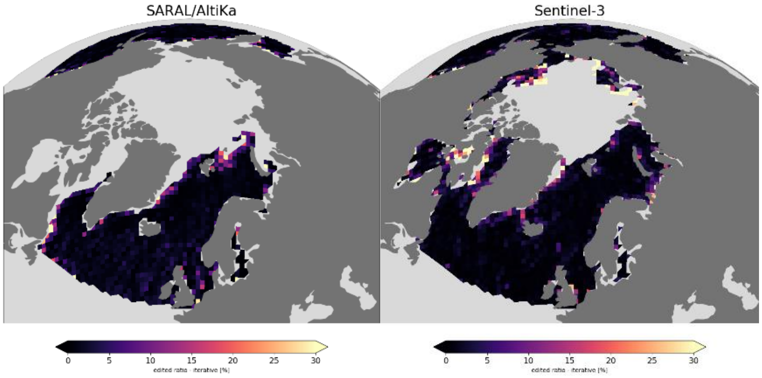

Figure 6, ratio of edited measurements on open ocean areas by the iterative editing process for SARAL/AltiKa and Sentinel-3, expressed in percentage.

7.4. Time/space editing

As a last editing step, we perform a spatio-temporal statistical editing. This is based on the estimation of local SLA statistics (mean and variance). Any measurement that is too far away from the expected distribution is removed. This does account for local seasonal cycle amplitude and phase to prevent removing summer/winter values systematically. While the ratio of measurements edited at this step is low, it does remove a few tracks with large offsets that were not flagged by previous editing steps, as well as some measurements in coastal areas.

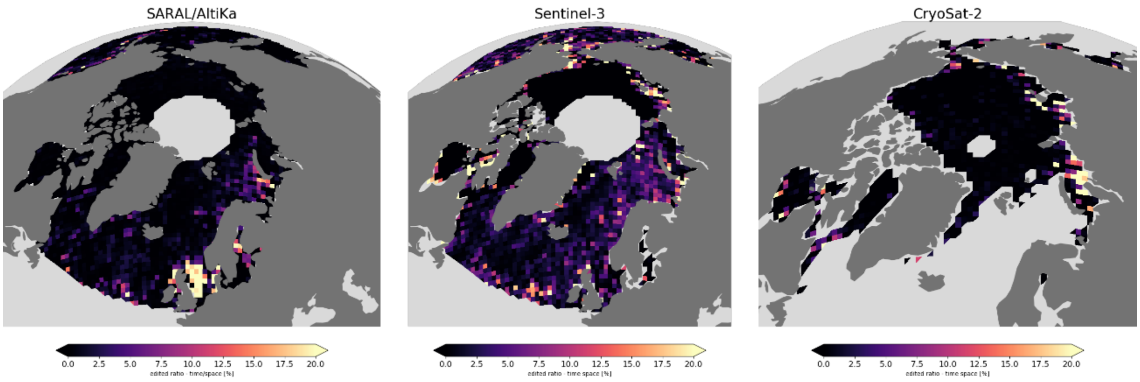

Figure 7, ratio of edited measurement by the spatio-temporal editing for SARAL/AltiKa, Sentinel-3 and CryoSat-2, in percentage

8. Gridding process and product format

8.1. Gridding

For mono-mission analysis, we adopt a simple gridding scheme based on box-averages. The grid used follows the EASE2 standard and allows for a near-constant spacing over the area with little distortion and is a better choice for polar areas than a regular grid in cartesian coordinates.

The grid spacing is set at 75 km. At each time step, the average integrates 30 days of observation. Grids are estimated every 10 days, so two consecutive grids are not independent. Generally, this ensures that at least several tens of individual measurements fall within each grid cell. The average number of measurements falling into each grid cell is shown on Figure 8 for all three missions.

Measurements are weighed according to the time of observation following a tukey window, so measurements getting close to T0+/-15 days have lower weights in the average.

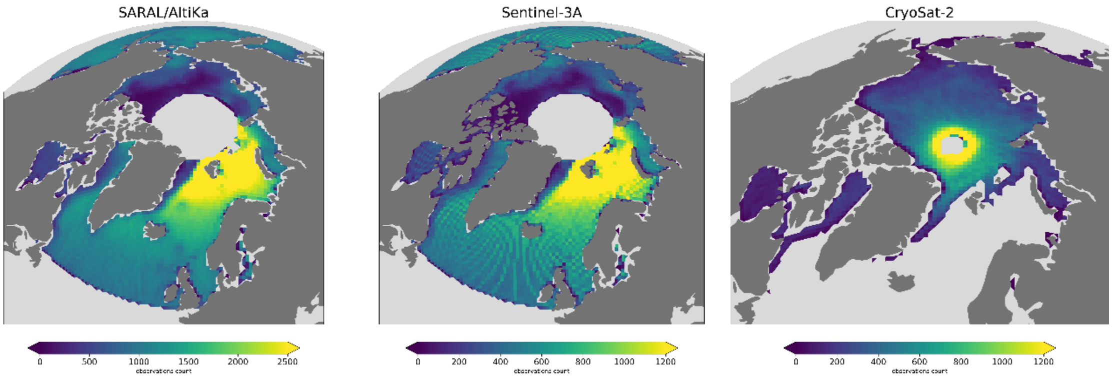

Figure 8, average number of valid observations in each grid cell for SARAL/AltiKa, Sentinel-3A and CryoSat-2

The grid spacing was set arbitrarily to balance resolution with coverage. Initially set to 100km, a short impact study showed that using 75km was possible with little cost in terms of coverage and SLA noise. With a 50 km grid some along-track correlated signals start to appear. At 25km, the resulting fields are very noisy and maps have large gaps. A grid spacing of 75km appears to provide a balance between Arctic coverage and noise level.

8.2. Product format

Gridded sea level anomalies are available as netCDF files. The format of the these files is briefly described below:

```
netcdf dataset {
dimensions:
      t = 102 ;
      x = 240 ;
```

```
      y = 240 ;
variables:
      float longitude(x, y) ;
            longitude:units = "degrees_east" ;
      float latitude(x, y) ;
            latitude:units = "degrees_north" ;
      float time(t) ;
            time:units = "days since 01-01-1950" ;
      float mean(x, y, t) ;
            mean:units = "m" ;
      float variance(x, y, t) ;
            variance:units = "m2" ;
      int number(x, y, t) ;
            number:units = "count" ;
}
```

Longitudes and latitudes define the lower left corner of each grid cell. Time is expressed in CNES decimal Julian days and corresponds to the central date of each averaging window.
Three variables hold the mean, variance and number of observations in each grid cell.

9. Open/ice-covered bias

For Sentinel-3A, we use two separate retrackings for the open ocean and the ice-covered areas. The processing discontinuity needs to be empirically corrected to estimate continuous SLA fields. The importance of this bias correction is illustrated on Figure 9 which shows a monthly mean SLA field for the open ocean and leads separately. Leads SLA appears to be biased high with respect to the surrounding open ocean.

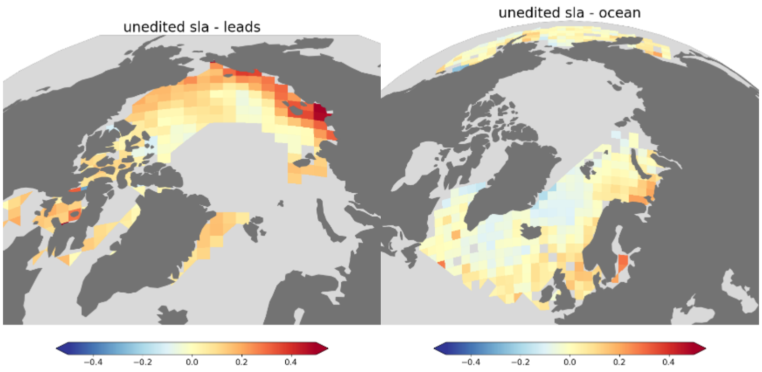

Figure 9, ocean and leads SLA for Sentinel3A before bias estimation

To correct for this bias, we estimate SLA from leads and open ocean in common grid cells for all months available, which is very similar to other publications (Armitage *et al.*, 2016). The geographical distribution of the mean and median bias is displayed on Figure 10, as well as the bias standard deviation.

The mean and median biases are close (around 16 cm). While the mean bias map shows a geographical distribution (higher bias Baffin Bay than around Fram strait for example), monthly biases maps (not shown) are noisy and do not show an obvious consistent pattern.
Over time (Figure 11) there is no sign of large bias variations (like a seasonal signal for example), yet large bias excursions are found (can be greater than 1.5m).
The open/ice-covered ocean bias is set to 16.6 cm, which corresponds to the mean bias value, after removal of high variability grid cells (Figure 10).

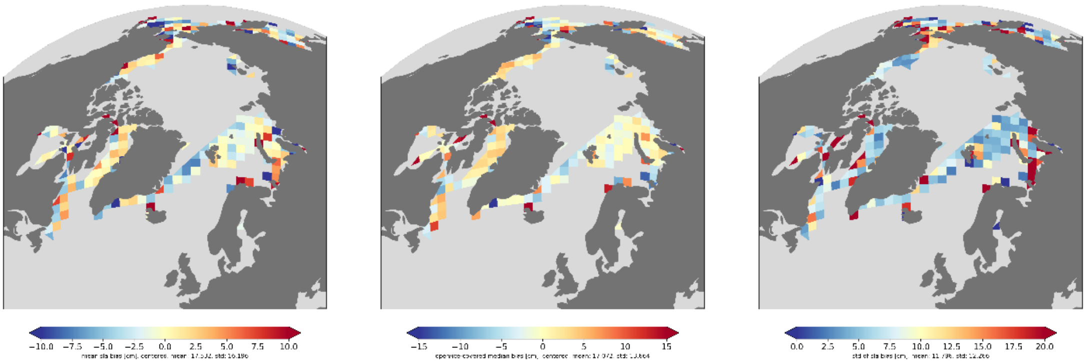

Figure 10, maps of the mean (left), median(center) and standard deviation (right) of the open/ice-covered SLA bias on Sentinel-3A

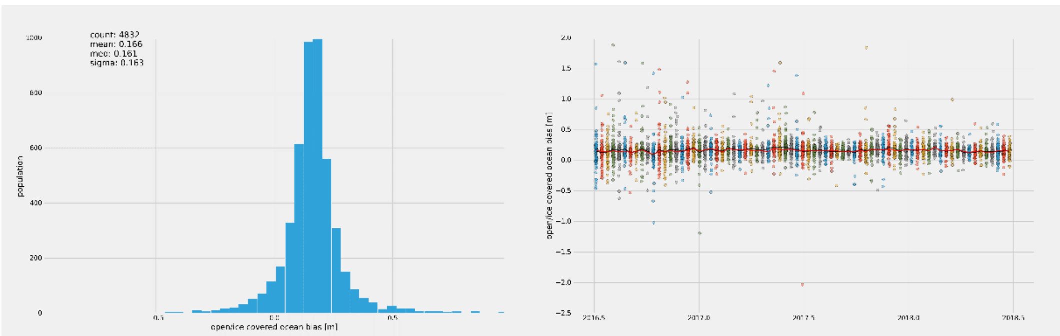

Figure 11, bias distribution (left) and evolution over time (right)

Applying this bias to Sentinel-3 data results in the map of Figure 12 (left), which does not exhibit any obvious bias at the transition with sea ice in the northern Atlantic Ocean. Integration over the whole period similarly does not indicate any remaining offset.
However, looking at SLA differences between missions (Figure 13) suggests that an open/ice-covered oceans bias remains in either Sentinel-3A or SARAL/AltiKa (or both).
Analysis of SARAL/AltiKa versus Sentinel-3A differences suggests that the Sentinel-3A bias is certainly closer to 11 cm than the 16.6 cm estimated by the above described method. In the following sections of this report, and in the final Sentinel-3A dataset, we use a 11 cm bias.

This is an important limitation in our current processing: given the available data sampling, we are unable to estimate accurately the bias between the open ocean and ice-covered areas. More importantly, this inaccuracy remains invisible in mono-mission analysis and is revealed by cross-comparisons only.

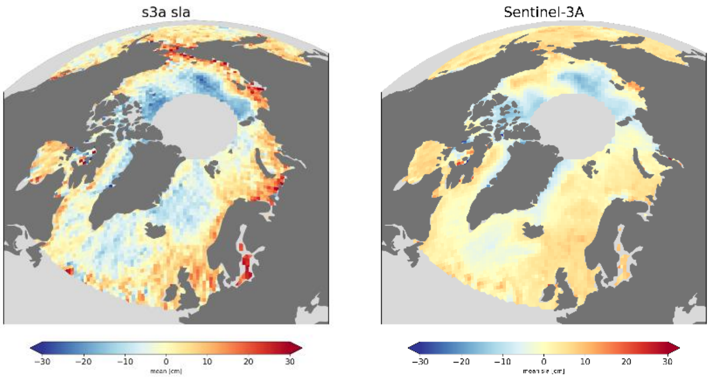

Figure 12, SLA maps from Sentinel-3A data over one month (left) and averaged over the whole period (right) after application of the 16.6 cm bias between open ocean and ice-covered areas

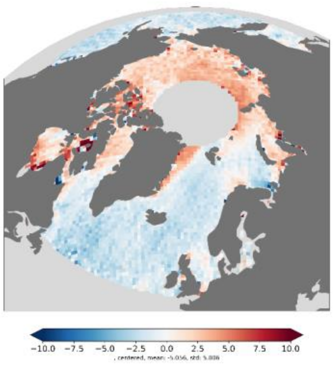

Figure 13, mean sea level difference between SARAL/AltiKa and Sentinel-3A

10. Validation

Sea level validation in the Arctic Ocean is difficult: in-situ data is scarce, numerical models often fail at representing the ocean under the ice… The validation results presented here mainly rely on macroscopic indicators, and are more qualitative than quantitative: are the main features of the Arctic Ocean circulation and variability correctly represented in the data? are the different missions consistent?

10.1. Geographical distribution

Looking at mean SLA maps provides a first validation result. The main features of the large-scale Arctic Ocean circulation should be correctly observed. The figure below shows the mean SLA maps for all missions over the longest period available for each mission. All missions see consistent large-scale features, despite apparent large-scale biases between them. A typical feature is the Beaufort Gyre which does appear consistently on all missions.

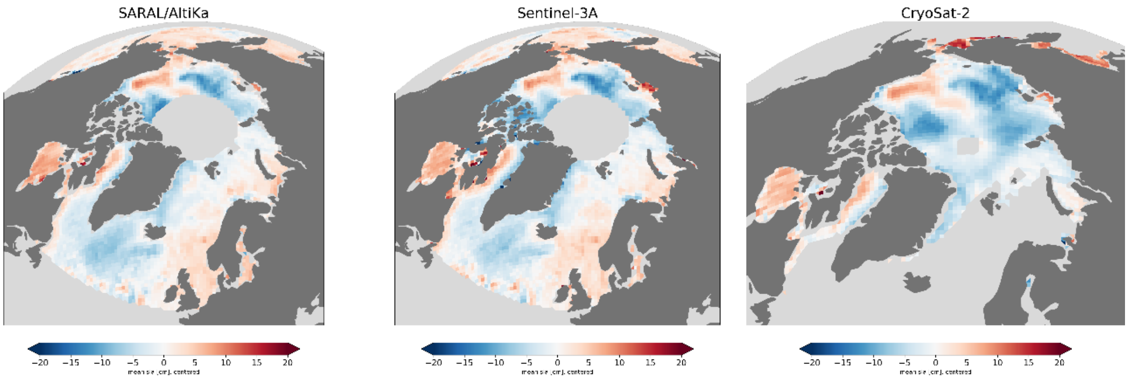

C

Figure 14, mean SLA maps over the Arctic Ocean, all maps were centered before plotting

Variance maps also provide a qualitative validation of the SLA fields: we don't expect large variance levels in the deeper parts of the Arctic Ocean. Variability should be trapped at the coast, as a response of the ocean to the wind forcing (eg. Proshutinsky *et al.*, 1997, RD 3). If high variability levels are observed in the Arctic Ocean interior, it might suggest that we were not able to properly identify lead echoes and that returns from leads and from the top of the ice are mixed together. Variance levels and distributions are very consistent from one mission to another. Low variance levels are observed in the interior of the basin, and higher variances are observed when getting closer to the coast, which is consistent with simple ocean circulation models. This is especially true along the Russian Arctic and in the shallower parts of the Siberian Arctic.
However we cannot rule out that these high variance levels result from processing errors:

- Tidal errors in these shallow areas,
- Lead discrimination in areas of fast ice.

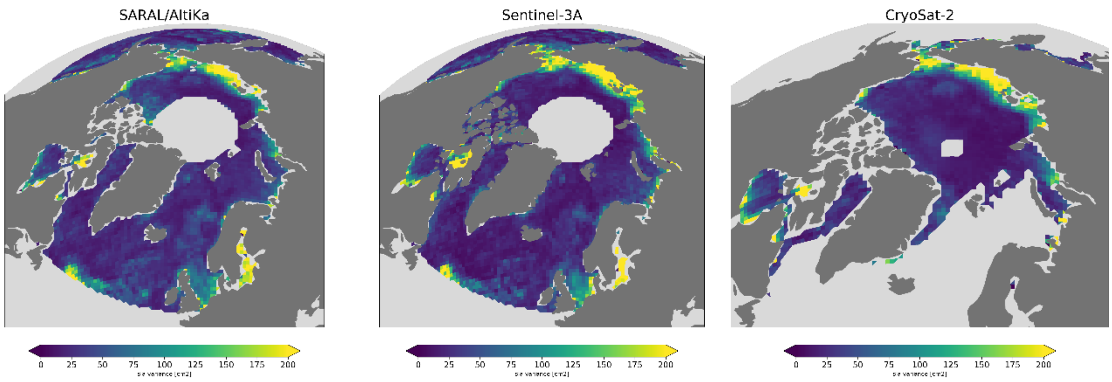

Figure 15, maps of SLA variance over the Arctic Ocean

10.2. Regional averages

Averaging sea level over the whole basin leads to an estimate of the regional Arctic Ocean sea level. Raw CryoSat-2 presents a large regional bias of about 1.15 m, CryoSat-2 SLA being lower than SARAL/AltiKa. A smaller bias is found between SARAL and Sentinel-3A (around 10 cm). All timeseries presented here are centered before plotting.
Figure 16 displays time series of the regional average Arctic Ocean sea level, first for the whole available domain of each mission (right). Sentinel-3A and SARAL/AltiKa are in excellent agreement, of course the signal is dominated by the annual signal, but even short-term variations are consistent.
CryoSat-2 appears off-tracks at first but reducing the averaging area to the one covered by CryoSat-2 (Figure 16, right) shows that over the ice-covered ocean which is tracked by CryoSat-2 SAR mode mask, all three missions show very consistent signals.

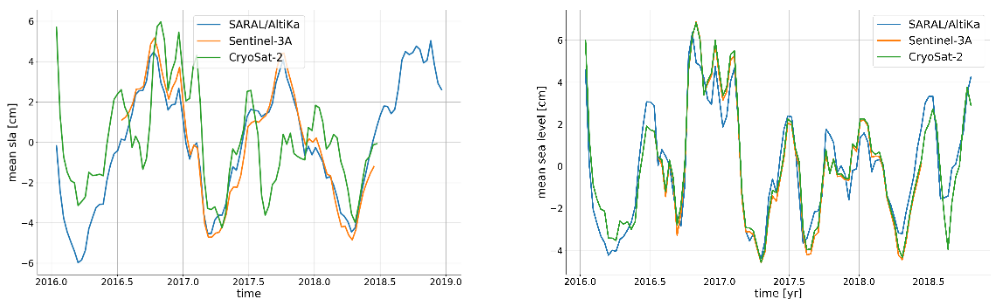

Figure 16, time series of Arctic Ocean average sea level (right) and estimated over the same area for all missions (left).

10.3. Cross-comparisons

For the first time, three overlapping missions are available over the Arctic Ocean. This is an opportunity for investigating inter-mission SLA differences. In this section we will use SARAL/AltiKa as a reference. This is the only mission that follows a homogeneous processing from open to ice-covered ocean. Furthermore, previous data quality assessment performed in the frame of the PEACHI project has shown its performance in the Arctic Ocean.

10.3.1. SARAL/AltiKa versus Sentinel-3A

Figure 17 displays the mean and variance of SLA maps differences between SARAL/AltiKa and Sentinel-3A. There is an excellent agreement between the two missions regarding the large scale mean sea level distribution. Differences remain well below 5 cm in most of the basin. Larger differences are found in coastal areas such as the Canadian Arctic Archipelago for example. There are however spatially consistent differences of smaller amplitudes, in the multiyear ice region for example, or north of Scandinavia.

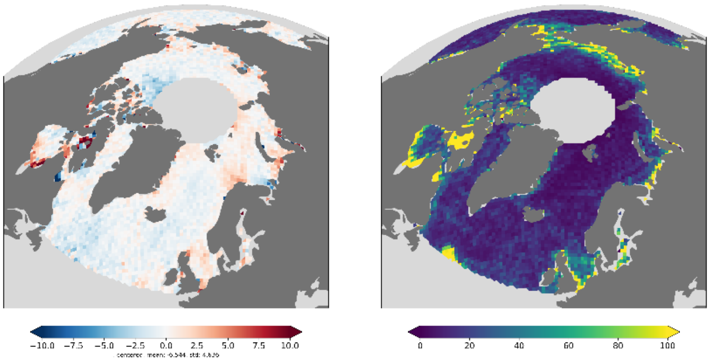

Figure 17, mean (left) and variance (right) of SLA differences between SARAL/AltiKa and Sentinel-3A

Regarding variance of SLA differences, low variance levels are found in the deep Arctic Ocean, which indicates that event in almost permanently ice-covered areas, the two altimeters measure similar sea levels. Discrepancies between the two missions are mainly found at the coast, where we expect data quality to be lower from degraded geophysical corrections mainly.

10.3.2. SARAL/AltiKa versus CryoSat-2

Comparing CryoSat-2 to SARAL/AltiKa shows a similar picture: mean sea level differences are generally lower than 5 cm in the Arctic Ocean, with slightly higher differences found at the coast (Figure 18). Again, high variance of the differences is observed mainly at the coast.

Both cross-comparisons show higher variance of SLA differences in the multiyear ice area (north of the Canadian Arctic Archipelago). In this area, sea-ice characteristics are very different than in first-year ice areas. There is a chance that our data classification and lead identification processes, as well as the editing process, could perform less accurately there.

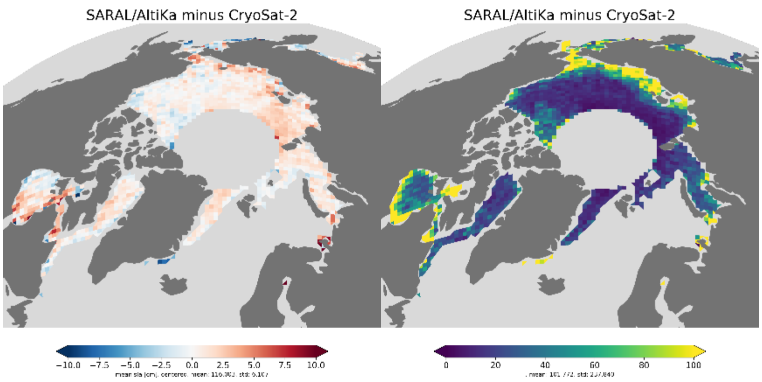

Figure 18, mean (left) and variance (right) of SLA differences between SARAL/AltiKa and CryoSat-2

10.4. Against DTU dataset

DTU produced the official SL-CCI dataset for the Arctic Ocean based on ALES+ retracking applied on ERS-1, ERS-2, Envisat and CryoSat-2 data (Rose et al., 2019, RD 4). This dataset covers the 2016-2018 period and is therefore suitable for comparison with our data.
Figure 19 displays the mean and variance of sea level anomalies derived from the DTU dataset over the 2016-2018 period. Geographical patterns are very similar regarding the mean sea level. The DTU dataset however has lower variance levels than our mono-mission products. This is likely a consequence of the objective analysis scheme they are using to map sea level anomalies.

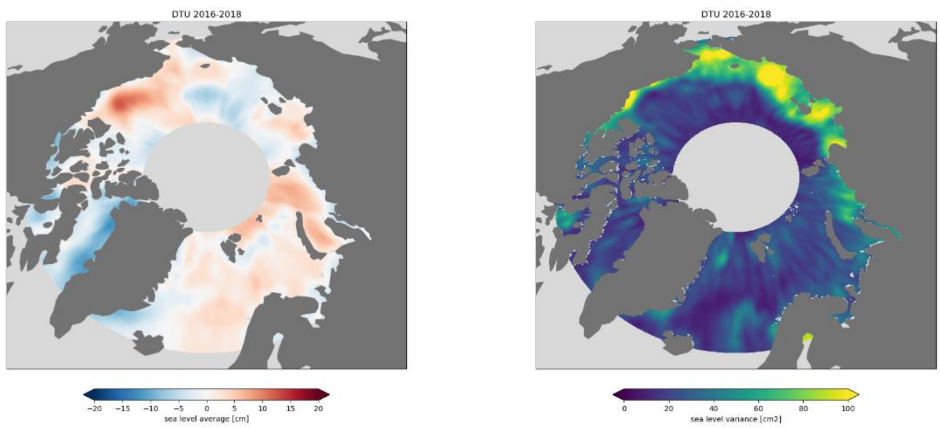

Figure 19, mean (left) and variance (right) of Arctic Ocean sea level anomalies from the DTU dataset over the 2016-2018 period

10.5. Against tide gauges

Tide gauges are a natural way to validate altimeter sea levels. In the Arctic Ocean however, tide gauges stations are scarce especially over such a short period.
Here we use PSMSL monthly data to perform our comparisons. These low-resolution data match well with the monthly temporal resolution of the altimeter gridded product.
Figure 20 qualitatively compares variance levels from tide gauges and altimetry. First there are very few data in the Arctic Ocean itself, were we expect improvements from the dedicated processing described in this report.
Tide gauges generally show higher variance levels than altimeter measurements, but some patterns are consistent, like a higher sea level variance in the Baltic Sea than along the Norwegian coast.

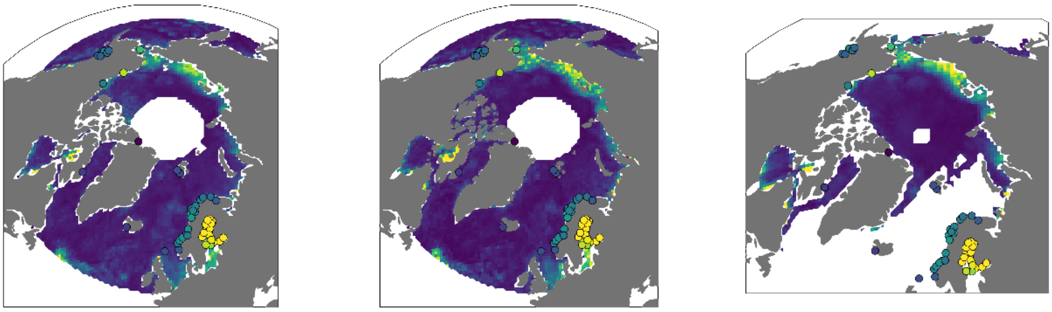

Figure 20, comparisons between sea level variance levels from altimetry (background) and tide gauges (overlaid dots) for SARAL/AltiKa (left), Sentinel-3A (center) and CryoSat-2 (right)

Direct time series comparisons show good agreement at most stations, three examples a given in Figure 21. It is hard to draw quantitative conclusions from these sets of comparisons. Variabilities seem to agree well in the Baltic Sea, in the North Atlantic and Pacific oceans, but there are too few stations, and too few measurements from stations in the Arctic Ocean basin itself to build reliable statistics.

FORM-NT-GB-7-1

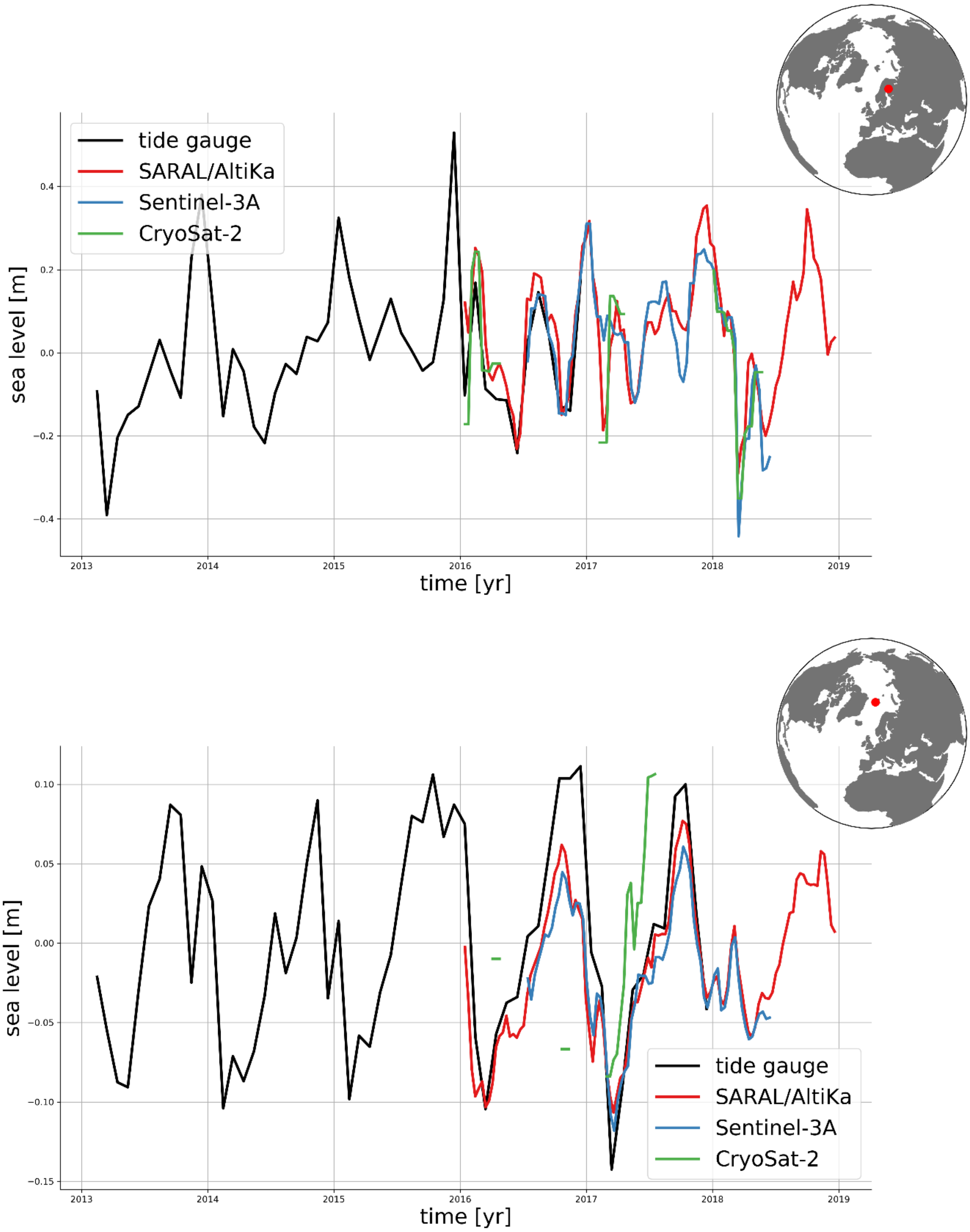

Figure 21, time series comparisons of sea levels from in-situ and altimeter at two different stations.

11. Conclusions

Based on previous work on sea level anomaly and ongoing studies on radar altimeter data over ice-covered surfaces, we were able to derive sea level anomaly maps for the Arctic Ocean covering (almost) three years and three missions (SARAL/AltiKa, Sentinel-3A and CryoSat-2).

We were able to apply the processing developed on Envisat and SARAL/AltiKa to SAR altimetry with minor changes and consistent results across missions. The final product is a series of gridded sea level anomaly maps with a 75km spatial resolution and monthly temporal resolution.

Cross-comparisons between missions are performed for the first time and reveal that all three missions observe consistent mean sea level patterns:

- Positive sea level anomaly in the Beaufort Gyre,
- Negative sea level anomaly in the Russian Arctic,
- Positive sea level anomaly in Hudson Bay,

and consistent sea level variability levels over the available period.
However, differences between datasets show that correcting the open/ice-covered ocean bias resulting from the non-continuous processing (different retracking algorithms) on Sentinel-3A is difficult from mono-mission data only. This advocates for using a homogeneous processing on all missions.

Validation to external reference data remain difficult and only provide qualitative results. Yet such comparisons (a satellite altimetry dataset from DTU and PSMSL tide gauge data) suggest that the grids generated here are reliable and represent correctly the large-scale variability of the Arctic Ocean.

Arctic Ocean data quality would certainly benefit from improvements at various levels of the processing chain:

- Homogeneous SAR waveform processing,
- Improvement of geophysical corrections (such as tides, mean sea surface, …),
- Improved editing of leads measurements, for example trying to discriminate melt ponds

List of acronyms

TBC	To be confirmed
TBD	To be defined
AD	Applicable Document
RD	Reference Document